Int J Adv Manuf Technol (2013) 66:1931–1941
DOI 10.1007/s00170-012-4471-y

ORIGINAL ARTICLE

Investigation of heat partition in dry turning assisted by heat pipe cooling

Liang Liang · Yanming Quan

Received: 12 April 2012 / Accepted: 14 August 2012 / Published online: 31 August 2012

Abstract Dissipation of the cutting heat through the cutting tool assisted by the heat pipe is a new cooling method in metal cutting. However, as an important indicator to evaluate the cooling performance, the heat partition in the cutting process for the heat pipe cutter has not been reported in the previous publications. This investigation is concerned with the estimation of the amount of heat flowing into the heat pipe cutter and that dissipated by the heat pipe. The aim is to characterize the heat partition of the heat pipe cutter and thus evaluate its cooling performance. Experimental results are presented of temperature measurements at the accessible positions on the cutter during orthogonal cutting. With these measured temperatures, the finite different methods and an inverse procedure are utilized to solve the heat flux loaded on the tool–chip interface and the amount of heat flowing into each part of the heat pipe cutter. It is shown that the installation of the heat pipe increases the heat flowing into the tool; however, much greater amount of heat can be dissipated by the heat pipe; this results in the reduction of the temperature at tool–chip interface.

Keywords Cutting tool · Heat pipe · Cutting heat · Heat partition · Inverse method

Nomenclature

L_h	The heated length in the evaporator section of the heat pipe (in millimeter)
L_c	The cooling length in the condenser section of the heat pipe (in millimeter)
α	The bending angle (in degree)
T_w	Temperature of the recycled water used in the cooling system (in Kelvin or degree Celsius)
v_c	Cutting speed (in meters per minute)
a_p	Depth of cut (in millimeter)
f	Feed (in millimeters per revolution)
T	Temperature (in Kelvin or degree Celsius)
k	Thermal conductivity (in watts per meter·Kelvin)
ρ	Density (in kilograms per cubic meter)
c	Specific heat (in joules per kilogram·Kelvin)
q_0	Intensity of inner heat source (in watts per cubic meters)
h	Surface convective heat transfer coefficients (in watts per square meter·Kelvin)
h_{cs}	The surface heat transfer coefficient between the heat pipe condenser and the recycled water (in watts per square meter·Kelvin)
$w(t)$	Heat flux loaded on the tool–chip interface (watts per square meter)
$Y_m(t)$	The measured temperature reading at the locations (x_m, y_m, z_m) of the cutter (in Kelvin or degree Celsius)
$T_m[w(t)]$	The simulated temperature at the location (x_m, y_m, z_m) with respect to the assumed heat flux magnitude $w(t)$ (in Kelvin or degree Celsius)
$J_m(w_n)$	The least square error between $T_m(w_n)$ and $Y_m(t)$
t_c	Cutting time (in second)
M	Number of measured temperature extracting points
Q_f	The work done in the secondary deformation zone along the tool rake face (in joule)
F_γ	The force component along the rake face, (in newton)
Λ_{ha}	The chip thickness ratio
γ_0	The rake angle (in degree)
F_c	The main cutting force (in newton)

L. Liang (✉) · Y. Quan
College of Mechanical and Automotive Engineering, South China University of Technology,
Guangzhou 510640, People's Republic of China
e-mail: double_double@163.com

F_f	The axial cutting force (in newton)
A_c	The tool–chip contact area on the insert (in millimeter)
E_{stored}	The rate of the heat stored within the control volume (in joules per second)
q_x	The heat conduction rate entering the control volume from x direction (in joules per second)
q_{x+dx}	The heat conduction rate existing the control volume from x direction (in joules per second)
E_q	The heat generated within the control volume (in joules per second)
$(T^{n+1}-T^n)$	The temperature variation between the increment $n+1$ and n
Q_{th}	The amount of heat stored in the toolholder (in joule)
S_n	The total time increment
E_n	Total number of the grids of the toolholder
Q_{hp}	The amount of heat dissipated by the heat pipe, (in joule)
V_w	The volume of water used in the cooling system, (in cubic millimeter)
E_s	The rate of the heat dissipated through the surface of the heat pipe condenser (in joules per second)
β	The heat partition coefficient entering into the cutting tool due to frictional heat source
R_{hp}	The ratio of the heat dissipated by the heat pipe to the heat flowing into the cutting tool
R_{th}	The ratio of the heat retaining in the toolholder to the heat flowing into the cutting tool

1 Introduction

Metal cutting is associated with high cutting temperature and hence the thermal aspects of the cutting process have serious consequences for both the tool and workpiece [1]. In order to rapidly remove the cutting heat from the cutting zone, the flooded cooling method is usually utilized in traditional metal cutting. However, since the usage of cutting fluid seriously degrades the environment quality and increase the cost of machining, the reduction of conventional amounts of cutting fluid is strongly required in modern manufacturing processes [2]. Investigation of new type of green cooling method has been one of the emerging topics related to production engineering in recent years [3].

The cutting tool assisted by heat pipe cooling presents an effective choice of green cooling in the cutting process. A heat pipe is a highly efficient heat conductor in which the latent heat of evaporation is used to transport great amount of heat in the presence of only small difference in temperature. In addition, the heat pipe can operate without the need for external power supply [4]. These unique properties suggest that the heat pipe should be an ideal device for removing the heat from a cutting tool.

In recent years, the investigation related to the cutting tool with heat pipe cooling has been carried out. Jen et al. have carried out the experimental and numerical investigation to verify the feasibility and effectiveness of heat pipe cooling in drilling operations; the results demonstrated that using a heat pipe in the drilling process can effectively extend the tool life of the drill [5–7]. Judd et al. [8] developed a turning tool with a round heat pipe embedded in the toolholder and experimentally demonstrated that the heat pipe helps to reduce the thermal elongation of the toolholder. By using the experimental method and finite element analysis, Haq and Tamizharasan [9] found that the installation of a heat pipe in the toolholder decreases the temperature at tooltip. Chiou et al. [10] also numerically verified that the cutting temperature can be reduced by using a turning tool with a heat pipe embedded in its insert. The similar conclusion could be found in the work carried out by Chou and Liu [11]. Based on the inverse heat conduction method, the author and co-researchers [12] have quantitatively investigated the tool–chip interface temperature of the cutter with a flat heat pipe attached on the insert rake face. The calculated results also show that the tool–chip interface temperature could be reduced for the cutter with heat pipe cooling.

As for the heat pipe cutter, external cooling will decrease its total thermal resistance and modify the heat partition of the rake face heat source. Cooling will affect cutting temperature in two ways. On one hand, cooling enhances the heat dissipation of the tool, which reduces the tool surface temperature. On the other hand, cooling will increases the heat flowing into the tool and hence increases the cutting temperature [13]. Therefore, determination of the heat partition of the heat pipe cutter is of particular interest to understand the effect of external cooling on the cutting temperature, but the relevant research has not been found in previous literatures.

This paper explores the characteristics of the cutting heat partition for the turning tool with heat pipe cooling. The focus of this work is to quantitatively estimate the amount of heat flowing into the cutting tool and that dissipated by the heat pipe. To achieve this, a combination of experiment measurements and numerical analysis was adopted. The temperatures at the accessible locations on the cutting tool were measured experimentally using the artificial

thermocouple method. With these measured temperatures, the finite different methods and an inverse procedure are utilized to solve the heat flux loaded on the tool–chip interface and the amount of heat flowing into each part of the cutting tool. The results in turning of AISI-1045 steel in different cutting speeds are presented.

2 Experimental details

2.1 The cutter with heat pipe cooling

The common cutter and the cutter with heat pipe cooling used for the investigation are shown in Fig. 1. The common cutter used for the investigation is constituted by a P10 carbide (WC–15 %TiC–6 %Co) insert, an insert fixture and a toolholder. The cutter with heat pipe cooling was designed and fabricated based on the common cutter. To install the heat pipe, a blind hole with a diameter of 6 mm and depth of 18 mm, which locates at 2 mm away from the tool tip, was EDMed in the insert. To reduce the thermal contact resistance between the heat pipe and the blind hole in the insert, the contact surface of the heat pipe was polished and the high-thermal conductivity grease was applied to the contact surface. In addition, the condenser section of the heat pipe was deviated from the toolholder to prevent the heat transfer between them.

The heat pipe used in this cutter was a round copper–water heat pipe with a diameter of 6 mm and length of 150 mm. The thickness of the heat pipe was 0.65 mm, and there were 55 straight grooves with a depth of 200 μm and width of 150 μm in its inner wall. In order to obtain the best heat transfer performance, the using parameters of the heat pipe in water cooling condition were optimized before the design of heat pipe cutter, given as follows: the heated length in the evaporator section L_h=18 mm, the cooling length in the condenser section L_c=20 mm, the bending angle α=5°, and the temperature of the water used for cooling T_w=75 °C [14].

The P10 carbide insert of these cutters has a specific heat of 208 J/kg·K and a density of 11,700 kg/m^3, respectively, while those of the toolholder and insert fixture are 473 J/kg·K and 7,801 kg/m^3, respectively. The temperature-dependent thermal conductivity of the insert and the toolholder are listed in Tables 1 and 2, respectively.

2.2 Experimental setup

The test setup used in the cutting experiments is shown in Fig. 2a. The cutting tests were conducted on a CNC turning lathe and performed dry. As for the heat pipe cutter, a recycled water cooling system was mounted on the condenser section of the heat pipe to remove the cutting heat and calorimetrically measure the cutting heat dissipated by the heat pipe. The cooling system consists of a recycled water container, a thermos container, two insulation hoses, and a submersible pump. The volume and the initial temperature of the water used in this system were 1 L and 75 °C, respectively, and the water flowing rate was fixed as 0.5 L/min.

The stand-alone temperature measurement system used in the cutting test constituted six artificial K-type thermocouples and a NI temperature acquisition module 9213. The schematic illustration of the temperature extracting positions on the cutters is shown in Fig. 2b. As for the common cutter, TC1 and TC3 are both on the rake face of the insert with TC1 close to and TC3 away from the tool tip, the position of TC2 locates on the flank face of the insert, and TC4 is placed on the toolholder. As for the heat pipe cutter, TC1 and TC2 are located on the insert rake face and flank face, respectively, while the TC3 and TC4 are placed on the evaporator section and condenser section of the heat pipe, respectively. In addition, TC 5 and TC6 locate in the recycled water container and the thermos container, respectively, as shown in Fig. 2a. A typical sample of the measured temperature at TC1, TC2, TC3, and TC4 on the heat pipe cutter and the measured temperature at TC5 and TC6 in the recycled water cooling system are presented in Fig. 3a, b, respectively.

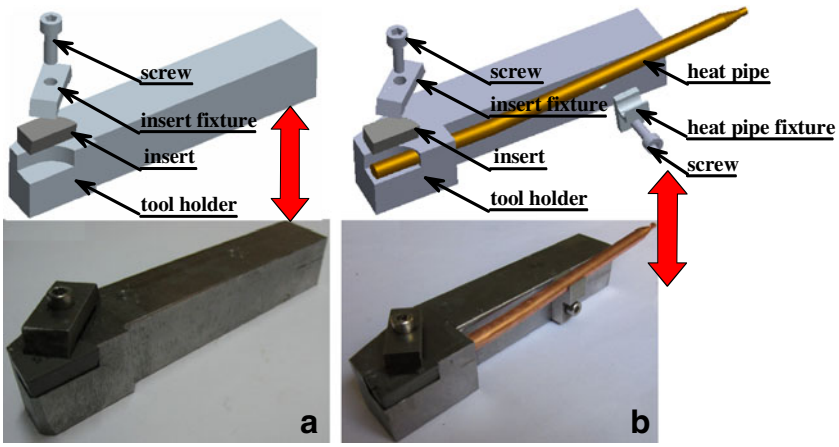

Fig. 1 Schematic illustration of **a** common cutter and **b** the cutter with heat pipe cooling

Table 1 Temperature-dependent thermal conductivity of the P10 carbide insert

Temperature (°C)	20	300	500	700	900	1,000	1,100	1,200
Conductivity (W/m·°C)	33.5	31.6	29.8	28.6	29.2	29.1	27.9	26.6

In order to compute the cutting power and further solve the amount of heat generated in secondary deformation zone in the cutting process, the cutting force was also measured in the cutting test. A Kistler cutting force dynamometer model 9265-A1 was used to measure the three-component cutting force. A typical cutting force sample is shown in Fig. 3c.

In addition, with the purpose of defining boundary condition at the tool–chip interface on the thermal model of the cutter, the coating method was applied to measure the actual tool–chip contact area on the insert in cutting process. According to this method, a layer of black paint with strong adhesive ability and a high melting point of 600 °C was evenly coated on the rake surface of the insert prior to the actual cutting test. After machining, the black paint on the tool–chip contact area would be scraped off, and the tool–chip interface can be measured and recorded by a tool microscope with video camera. A typical image of the tool–chip interface taken by the coating method is presented in Fig. 3d.

The workpiece used in the experiment was an AISI-1045 steel cylindrical rod with a length of 500 mm and a diameter of 100 mm. The experiments were conducted by varying the cutting speed v_c from 100 to 300 m/min with the fixed cutting depth a_p=1.6 mm and feed rate f=0.15 mm/rev. For all cut, the cutting time t_c was kept constant as 200 s.

3 Solution of heat flux on tool–chip interface

3.1 The 3D thermal model of cutters

The 3D thermal models of the common cutter and the heat pipe cutter were developed for the temperature simulation based on the predefined heat flux on the tool–chip contact area. Figure 4 shows the schematic view of the thermal models. By using temperature-dependent thermal properties, the 3D transient heat diffusion equation of these models in Cartesian coordinates can be written as:

$$\frac{\partial^2 T}{\partial x^2}+\frac{\partial^2 T}{\partial y^2}+\frac{\partial^2 T}{\partial z^2}+\frac{q_0}{k}=\frac{\rho c}{k}\cdot\frac{\partial T}{\partial t} \tag{1}$$

Where T is the temperature (in degree Celsius), k the thermal conductivity (in watts per meter·Kelvin), q_0 the intensity of inner heat source (in watts per cubic meter), ρ the density (in kilograms per cubic meter), and c the specific heat (in joules per kilogram·Kelvin).

As for the common cutter, the initial condition is:

$$T(x,y,z,0)=T_\infty \tag{2}$$

The boundary condition is:

$$-k\frac{\delta T}{\delta \eta}=h(T-T_\infty) \tag{3}$$

In Eqs. 2 and 3, T_∞ is the ambient temperature (in degree Celsius), $\delta T/\delta\eta$ the derivative of the temperature along the outward drawn normal to the surface, and h the convective heat transfer coefficients at the surface (in watts per square meter·Kelvin).

As for the cutter with heat pipe cooling, the initial condition is:

$$T(x,y,z,0)=\begin{cases} T_w \text{ (heat pipe)} \\ T_\infty \text{ (other components)} \end{cases} \tag{4}$$

Where T_w is the initial temperature of the recycled water in the cooling system.

The boundary condition is:

$$-k\frac{\delta T}{\delta \eta}=\begin{cases} h_{cs}(T_{cs}-T_w) \text{ (surface of the heat pipe condenser)} \\ h(T_s-T_\infty) \text{ (surface of other components)} \end{cases} \tag{5}$$

Where h_{cs} is the surface heat transfer coefficient between the heat pipe condenser and the recycled water. T_{cs} is the surface temperature of the heat pipe condenser. The relationship between h_{cs} and T_{cs} can be obtained from the heat pipe performance test [14], as shown in Fig. 5a.

The heat pipe was modeled as an entity with given physical and thermal properties, the effect of temperature on the effective thermal conductivity of the heat pipe is shown in Fig. 5b [14].

For both cutters, the boundary condition in the tool–chip contact area is:

$$-k\frac{\delta T}{\delta \eta}=w(t) \tag{6}$$

Table 2 Temperature-dependent thermal conductivity of the tool-holder and the insert fixture

Temperature (°C)	20	100	200	300	400	600
Conductivity (W/m·°C)	53.7	51.9	48.5	45.0	41.5	34.6

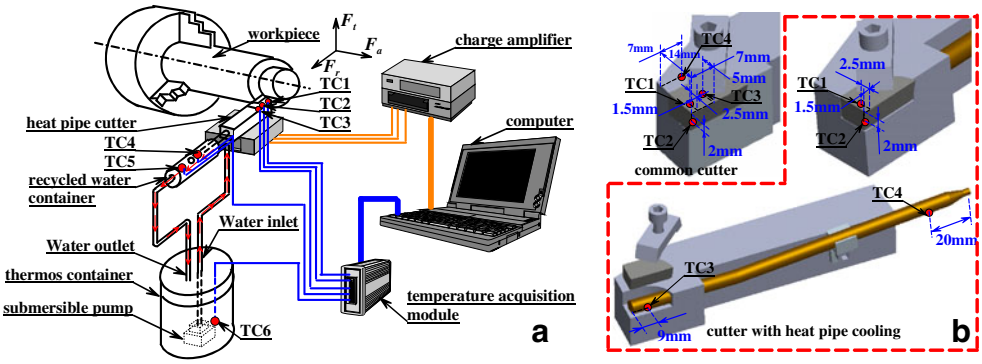

Fig. 2 Schematic illustration of **a** experimental setup and **b** temperature extracting positions on the cutters

Here $w(t)$ is the heat flux loaded on the tool–chip interface (in watts per square meter).

The tool–chip interfaces in these thermal models were defined according to the experimental measured results in Section 2.2. The thermal models were calculated by the software ABAQUS 6.8, and all case of the simulations were based on a constant time increment of 1 s for a cutting time of 120 s.

3.2 The inverse procedure

The solution of above models represents a direct problem, in which the heat flux loaded on the tool–chip interface must be predefined. Unfortunately, the heat flux over the tool–chip interface is difficult to obtain directly in the turning process.

In this work, based on the measured temperature on the accessible positions of the cutter in cutting process, the unknown effective heat flux $w(t)$ on the tool–chip interface in steady cutting was solved by an inverse algorithm. Assuming the distribution of heat flux on tool–chip interface is uniform, the objective function of the inverse procedure can be described as follows:

$$J[w(t)] = \int_{t=0}^{t_c} \sum_{m=1}^{M} \left\{ \begin{array}{r} T[x_m, y_m, z_m, t, w(t)] \\ -Y(x_m, y_m, z_m, t) \end{array} \right\}^2 dt$$

$$= \int_{t=0}^{t_c} \sum_{m=1}^{M} \{T_m[w(t)] - Y_m\}^2 dt \qquad (7)$$

Here, $Y(x_m, y_m, z_m, t)=Y_m(t)$ is the temperature readings using thermocouple taken at the appropriate locations (x_m, y_m, z_m) on the cutters, $T[x_m, y_m, z_m, w(t)]=T_m[w(t)]$ is the simulated temperature at the same locations with respect to the assumed heat flux magnitude $w(t)$, t_c denotes the cutting

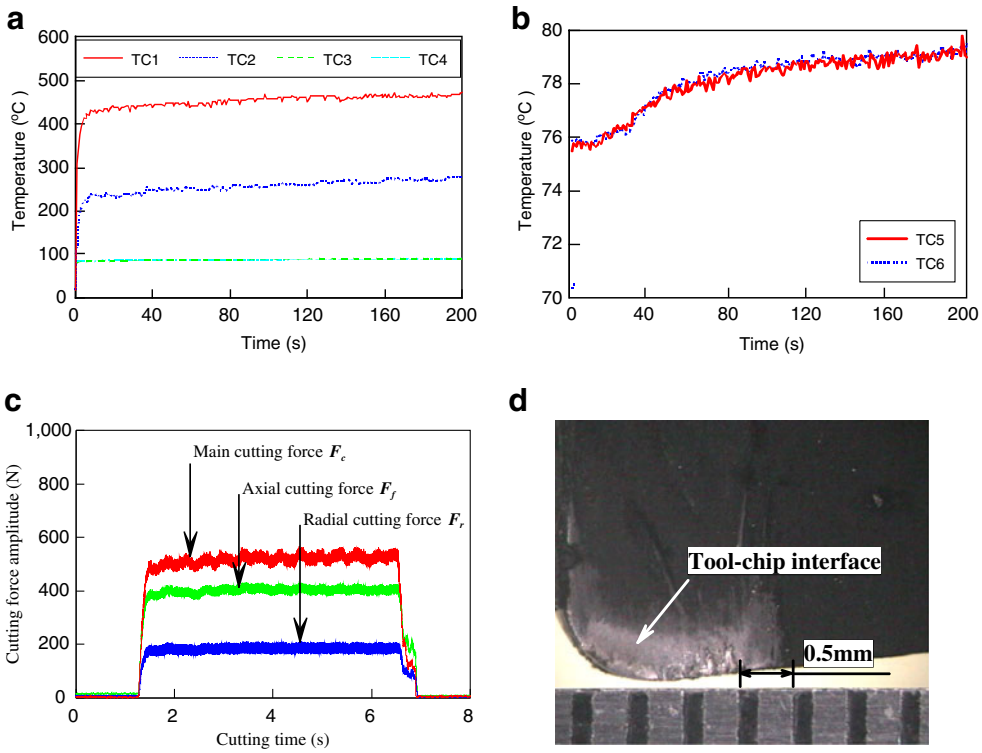

Fig. 3 The typical sample of **a** the measured temperature at TC1, TC2, TC3, and TC4 on the heat pipe cutter; **b** the measured temperature at TC5 and TC6 in the recycled water cooling system; **c** the cutting force signal for the common cutter; and **d** the view of tool–chip interface obtained by the coating method for the common cutter; (v_c=100 m/min, a_p= 1.6 mm, and f=0.15 mm/rev)

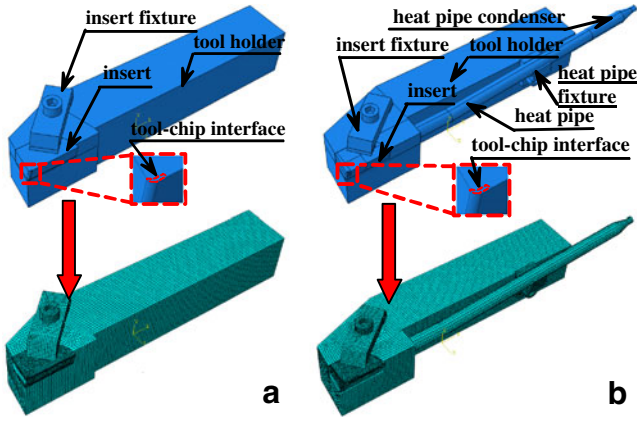

Fig. 4 The finite different models of **a** the common cutter and **b** the cutter with heat pipe cooling

time, and M denotes the number of measured temperature extracting points.

By optimizing the unknown heat flux $w(t)$ on the thermal model to minimize the objective function $J[w(t)]$, the effective heat flux on the tool–chip interface can be determined. In this work, the conjugate gradient method was utilized in the optimizing procedure. The corresponding optimizing algorithm was programmed by FORTRAN, and the data transformation between the optimizing code and ABAQUS 6.8 was established to solve above an inverse problem.

4 Solution of the heat flowing into each parts of the turning tool

4.1 The amount of heat generated in secondary deformation zone

Heat generation at the secondary deformation zone is mainly due to the friction in the tool–chip sliding contact. In this study, since the tool employed has a 0° inclination angle and 0° lead angle, with a depth of cut sufficiently larger than the feed and the tool nose radius, it is reasonable to apply orthogonal cutting mechanics for the heat source analysis.

According to the orthogonal cutting model developed by Shaw [15], the amount of heat generated due to the work done in the secondary deformation zone along the tool rake face is calculated by the following equation:

$$Q_{\mathrm{f}} = \left(F_{\gamma} v_{\mathrm{c}} / \Lambda_{\mathrm{ha}}\right) \cdot t_{\mathrm{c}} \tag{8}$$

Where F_{γ} is the force component along the rake face (in newton), v_{c} the cutting speed (in meters per second), Λ_{ha} the chip thickness ratio, and t_{c} the cutting time. The force F_{γ} could be calculated as follows:

$$F_{\gamma} = F_{\mathrm{c}} \sin\gamma_0 - F_{\mathrm{f}} \cos\gamma_0 \tag{9}$$

Whereγ_0 is the rake angle; F_{c} and F_{f} is the main cutting force (in newton) and axial cutting force (in newton), respectively, which could be obtained from the cutting force measurement test.

4.2 The amount of heat flowing into the cutting tool

Based on the effective heat flux magnitude $w(t)$ solved by the inverse procedure, the amount of heat flowing into the cutters through the tool–chip interface could be calculated as:

$$Q_{\mathrm{t}} = \int_0^{t_{\mathrm{c}}} w(t) \cdot A_{\mathrm{c}} dt \tag{10}$$

Here, t_{c} is the cutting time and A_{c} is the tool–chip contact area on the insert.

4.3 The amount of heat retaining in the toolholder

Based on the simulated results of the thermal models, the amount of heat retaining in the toolholders could be solved. The schematic illustration of the heat exchange of a hexahedral control volume in the toolholder is presented in Fig. 6. According to the first law of thermodynamics, the rate of the heat stored within the control volume E_{stored} is calculated by following equation:

$$\begin{aligned} E_{\mathrm{stored}} &= q_x + q_{x+dx} + q_y + q_{y+dy} + q_{z+dz} + q_z + E_{\mathrm{q}} \\ &= \rho_{\mathrm{th}} c_{\mathrm{th}} \Delta x \Delta y \Delta z (T^{n+1} - T^n)/\Delta t \end{aligned} \tag{11}$$

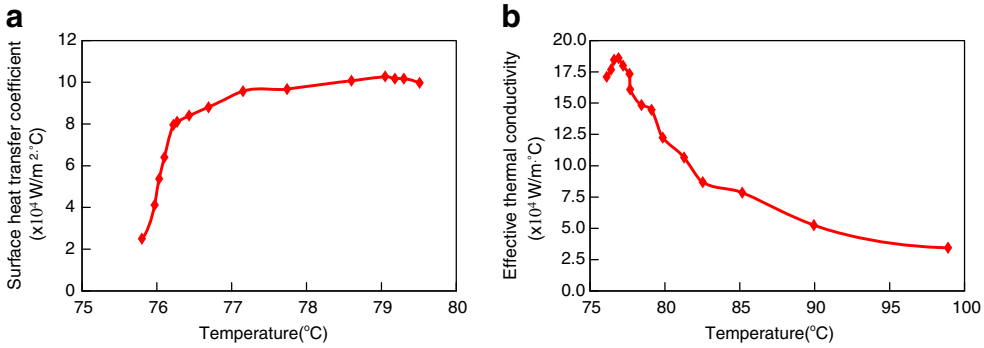

Fig. 5 The effect of temperature on **a** the surface heat transfer coefficient of the heat pipe condenser and **b** effective thermal conductivity of the heat pipe [14]

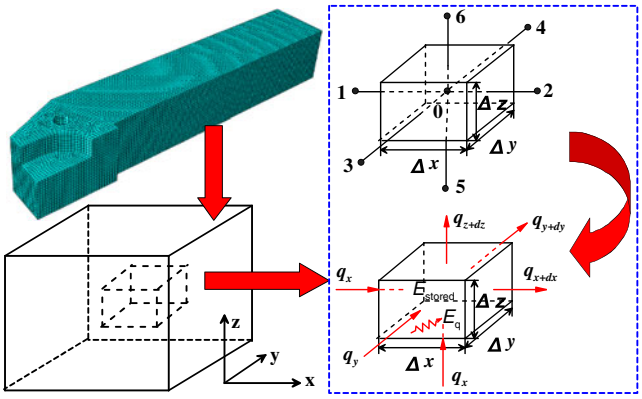

Fig. 6 Schematic illustration of the heat exchange of a control volume in the toolholder

Where, q_x, q_y, and q_z, denote the heat conduction rate entering the control volume from x, y, and z directions, respectively, while q_{x+dx}, q_{y+dy}, and q_{z+dz} denotes the heat conduction rate existing the control volume from x, y, and z directions, respectively. E_q is the rate of the heat generated within the control volume. ρ_{th} is the density of the toolholder, c_{th} the specific heat of the toolholder, and $(T^{n+1}-T^n)$ is the temperature variation between the increment $n+1$ and n.

According to Eq. 11, the amount of heat retained in the toolholder Q_{th} could be obtained from the simulated result of the thermal model, Q_{th} is given by following equation:

$$Q_{th} = \sum_{n=0}^{Sn-1}\sum_{i=0}^{En-1} E^n_{storedi}\Delta t = \sum_{n=0}^{Sn-1}\sum_{i=0}^{En-1} \rho_{th}\cdot c_{th}\cdot(\Delta x_i \Delta y_i \Delta z_i)\cdot(T_i^{n+1}-T_i^n) \quad (12)$$

Where S_n denotes the total time increment, E_n the total number of the grids of the toolholder, and i is the number of the grid.

4.4 The amount of heat dissipated by the heat pipe

Both the calorimetric method and the numerical method were utilized to measure the amount of heat dissipated by the heat pipe Q_{hp} in this study. The calorimetric method is based on the temperature measurement experiment in the Section 2.2. Assuming that the temperature variations at the positions of TC5 and TC6 in Fig. 2a are ΔT_5 and ΔT_6, respectively, Q_{hp} can be calculated according to following equation:

$$Q_{hp} = \rho_w \cdot V_w \cdot c_w \cdot (\Delta T_5 + \Delta T_6)/2 \quad (13)$$

Where ρ_w is the density of water, V_w the volume of water used in the cooling system, and c_w the specific heat of water.

Based on the simulated results of the thermal models of the heat pipe cutter, Q_{hp} also can be solved. The schematic illustration of the heat exchange of a control volume at the surface of the heat pipe condenser is presented in Fig. 7. According to the first law of thermodynamics, the rate of the heat dissipated through the surface of the heat pipe condenser E_s is calculated by following equation:

$$E_s = q_x + q_{x+dx} + q_y + q_{y+dy} + q_z - E_{stored} + E_q = h_{cs}\Delta x \Delta y (T_i^n - T_w)/\Delta t \quad (14)$$

Where, h_{cs} is the surface heat transfer coefficient between the heat pipe condenser and the recycled water and T_w is the temperature of the water.

Based on Eq. 14, the amount of heat dissipated by the heat pipe Q_{hp} can be calculated according to following equation:

$$Q_{hp} = \sum_{n=0}^{Sn-1}\sum_{i=0}^{Hn-1} E_{si}{}^n \Delta t = \sum_{n=0}^{Sn-1}\sum_{i=0}^{Hn-1} h_{cs}\cdot(\Delta x_i \Delta y_i)\cdot(T_i^n - T_w) \quad (15)$$

Where S_n denotes the total time increment, H_n the total number of the grids of at the surface of the heat pipe condenser, and i is the number of the grid.

5 Result and discussion

5.1 The heat flux and temperature at tool–chip interface

As described in Section 3.2, with the measured temperatures at the accessible positions on the cutter, the effective heat flux magnitude and the temperature at tool–chip interface can be solved based on the inverse procedure. As for the heat pipe cutter, the temperature obtained at TC1, TC2, and TC3 were used to establish the objective function of the inverse procedure, while the temperature measured at TC4

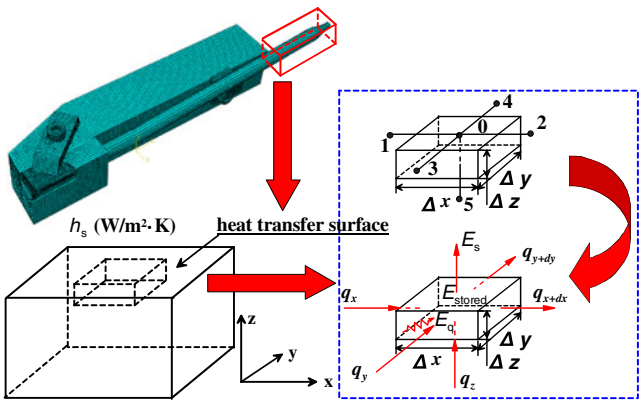

Fig. 7 Schematic illustration of the heat exchange of a control volume at the surface of the heat pipe condenser

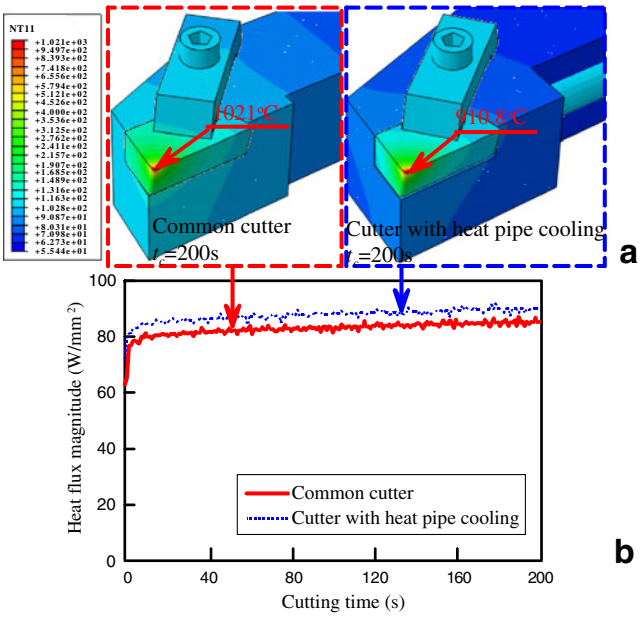

Fig. 8 The solved tool–chip interface temperature at the cutting time of 200 s and the estimated heat flux on the tool–chip interface in cutting process for two cutters. (v_c=200 m/min, a_p=1.6 mm, f=0.15 mm/rev)

was used as the purpose of verification. As for the common cutter, the temperature obtained at TC1, TC2, and TC4 were used to establish the objective function, while the temperature measured at TC3 was used as the checking temperature.

The estimated heat flux of the common cutter and heat pipe cutter at the cutting speed v_c=200 m/min are shown in Fig. 8b. It can be observed that the solved effective heat flux magnitude $w(t)$ for both cutters increase slightly with the cutting time in a steady cutting process, but the $w(t)$ for the common cutter is lower than that of heat pipe cutter. The solved temperature fields of the cutters at t_c=200 s with respect to the estimated heat flux are reported in Fig. 8a. It can be learned that the tool–chip contact area of the cutters have the highest temperatures. The maximum temperature at the tool–chip interface T_{max} for the common cutter is 1,021 °C, while that for the cutter with heat pipe cooling is 910.8 °C.

The comparison of the measured and estimated temperature at TC1, TC2, and TC3 of the heat pipe cutter at the cutting speed v_c=200 m/min is illustrated in Fig. 9a–c, respectively. It can be seen from these figures that they are in good agreement. The relative error at TC1, TC2, and TC3 is calculated as E_{T1}=3.84 %, E_{T2}=5.59 %, and E_{T3}=4.91 %, respectively, where E_{Tm} is defined as:

$$E_{Tm} = \left[\left(\sum_{t=1}^{200}\left|\frac{T_m(t)-Y_m(t)}{Y_m(t)}\right|\right)/200\right]\times 100\% \qquad (16)$$

In order to verify the accuracy of the present inverse algorithm, the temperature at TC4 is calculated by using the estimated heat flux. The comparison of the measured and calculated temperature at TC4 is plotted in Fig. 8d. The relative error is calculated as E_{T4}=2.12 %.

The measured and estimated temperatures at TC1, TC2, and TC4 of the common cutter at the cutting speed v_c= 200 m/min are illustrated in Fig. 10a–c, respectively. The comparison of the measured and calculated temperatures at TC3 is plotted in Fig. 10d. The relative errors at TC1, TC2, TC3, and TC4 are calculated as E_{T1}=4.12 %, E_{T2}=3.02 %,

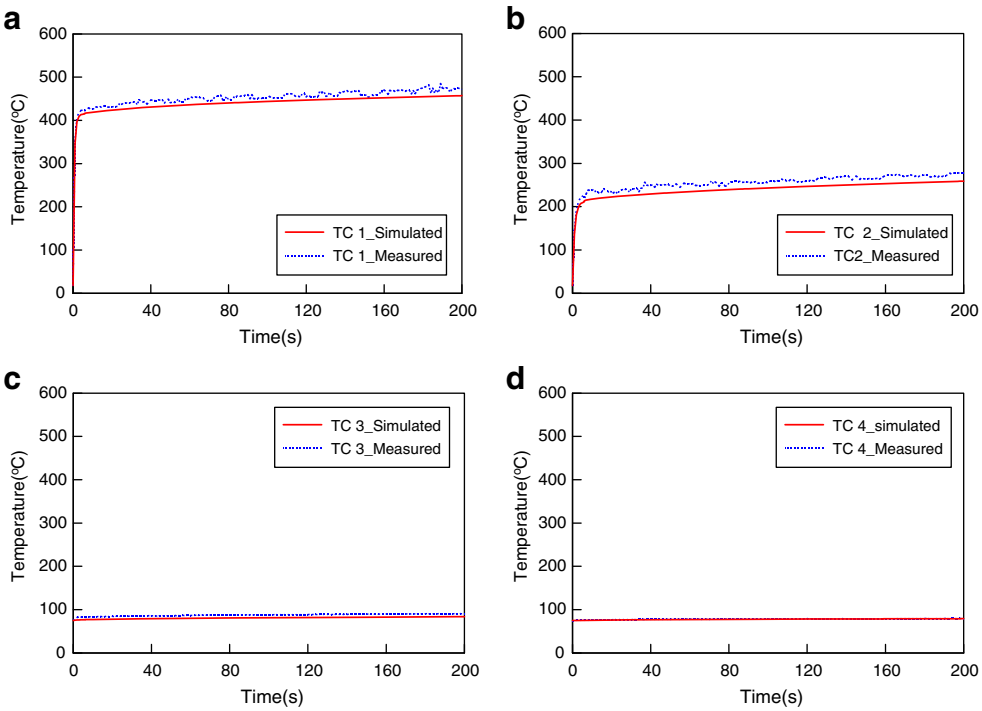

Fig. 9 The measured and estimated temperature of the heat pipe cutter at **a** TC1, **b** TC2, **c** TC3, and **d** the measured and calculated temperatures (using estimated heat flux) at TC4. (v_c=200 m/min, a_p=1.6 mm, f=0.15 mm/rev)

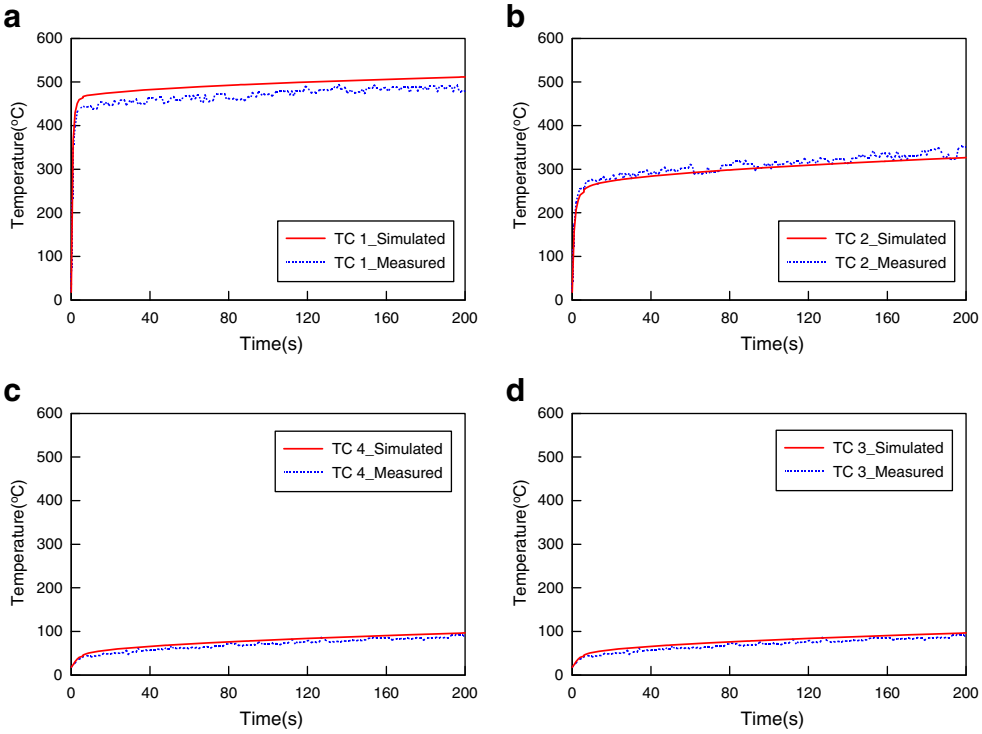

Fig. 10 The measured and estimated temperature of the common cutter at **a** TC1, **b** TC2, **c** TC4, and **d** the measured and calculated temperatures (using estimated heat flux) at TC3. (v_c=200 m/min, a_p=1.6 mm, f=0.15 mm/rev)

E_{T4}=5.11 %, and E_{T3}=5.62 %, respectively. This implies that the present estimated heat flux is indeed the actual drilling heat flux since the residual between the checking and measuring temperatures are always within the reliable range.

Figure 11a presents the effect of cutting speed on the average heat flux magnitude $\widehat{w}$ between the cutting time 100 to 200 s, where $\widehat{w}$ is defined as follows:

$$\widehat{w} = \left(\sum_{t=100}^{200} w(t) \right) / 100 \tag{17}$$

According to Fig. 11a, it can be seen that the value of $\widehat{w}$ increase with the cutting speed for both cutters, generally, $\widehat{w}$ for the cutter with heat pipe cooling is higher than that of common cutter, especially in high-speed region, 250–300 m/min.

The effect of the cutting speed on the maximum temperature at tool–chip interface T_{max} for two cutters is presented in Fig. 11b. It shows that T_{max} for both cutters increase gradually with the cutting speed increase. Generally, T_{max} of the common cutter is found to be significantly higher than that of heat pipe cutter in all cutting speeds. This implies that the heat pipe has a good cooling effect and it can be also found in Fig. 11b that the T_{max} of the common cutter is in good agreement with that reported by Zhou [16], who reported a similar cutting temperature trend using the tool work thermocouple method in the same cutting condition. This validates the accuracy of the inverse method used in this study.

5.2 Heat partition into each part of the cutters

The heat partition into the cutting tool due to frictional heat source at the secondary deformation zone, β, is defined as follows:

$$\beta = Q_t / Q_f \tag{18}$$

Here, Q_f is the amount of heat generated in secondary deformation zone, which can be obtained from Eq. 8 stated

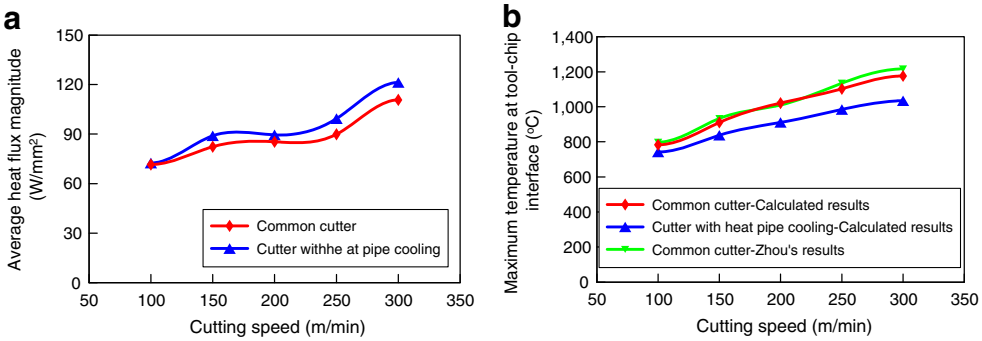

Fig. 11 The effect of the cutting speed on **a** the average heat flux magnitude and **b** maximum temperature at tool–chip interface

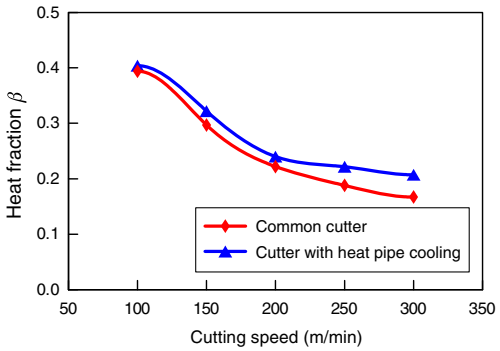

Fig. 12 The effect of the cutting speed on the heat partition to the cutting tool due to frictional heat source

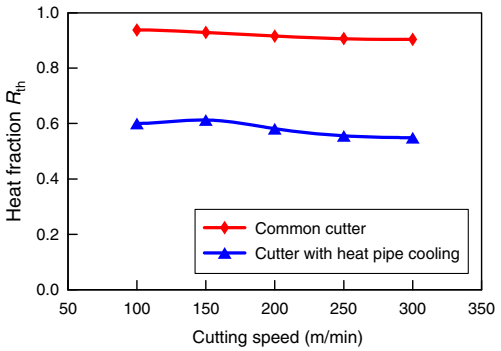

Fig. 14 The effect of the cutting speed on the ratio of the heat retaining in the toolholder to the heat flowing into the cutting tool for the common cutter and heat pipe cutter

in Section 4.1; Q_t is the amount of heat flowing into the cutting tool, which can be solved by Eq. 10 stated in Section 4.2. The effect of cutting speed on β for the common cutter and heat pipe cutter is presented in Fig. 12. It shows that the value of β decrease with the cutting speed increase for both cutters. This may be due to the fact that the shorter contact time between the tool and chip in higher cutting speed results in the reduction of cutting heat conducted into the tool. Furthermore, it can be also observed in Fig. 12 that the value of β for the heat pipe cutter is higher than that for the common cutter in all cutting speed. This means that the installation of the heat pipe increase the amount of heat flowing into the tool, which may be attributed to the relative lower thermal resistance of the heat pipe cutter.

As for the heat pipe cutter, the ratio of the heat dissipated by the heat pipe to the heat flowing into the tool, R_{hp}, is defined as follows:

$$R_{hp} = Q_{hp}/Q_t \tag{19}$$

Here, Q_{hp} is the amount of heat dissipated by the heat pipe in cutting process. The Q_{hp}, obtained from the numerical method and calorimetric method stated in Section 4.4, is shown in Fig. 13a. It is found that the numerical results have a good agreement with the calorimetric measured results in all cutting speed. This also validates the reliability of the thermal model of the heat pipe cutter.

Figure 13b presents the effect of cutting speed on R_{hp}. It shows that R_{hp} slightly decrease with increasing cutting speed from 100 to150 m/min, and increase gradually with cutting speed within the high-speed region, and reaches 42 % at 300 m/min. This means that 42 % of the cutting heat following into cutting tool can be dissipated through the heat pipe embedded in the cutting tool at the cutting speed of 300 m/min.

The ratio of the heat retaining in the toolholder to the heat flowing into the cutting tool, R_{th}, is defined as follows:

$$R_{th} = Q_{th}/Q_t \tag{20}$$

Here, Q_{th} is the amount of heat retaining in the toolholder, which can be calculated from Eq. 12 stated in Section 4.3. The effect of the cutting speed on R_{th} is presented in Fig. 14. It is observed that R_{th} for the common cutter is more than 90 % in all cutting speed, while that for the heat pipe cutter is much lower, only keep at 56–60 %. This implies that the heat pipe embedded in the cutting tool significantly reduces the heat retaining in the toolholder, especially in high cutting speed. It is can hence supposed that the installation of the heat pipe helps to reduce the thermal elongation of the toolholder.

Fig. 13 The effect of the cutting speed on **a** the heat dissipated by the heat pipe, and **b** the ratio of the heat dissipated by the heat pipe to the heat following into the cutting tool for the heat pipe cutter

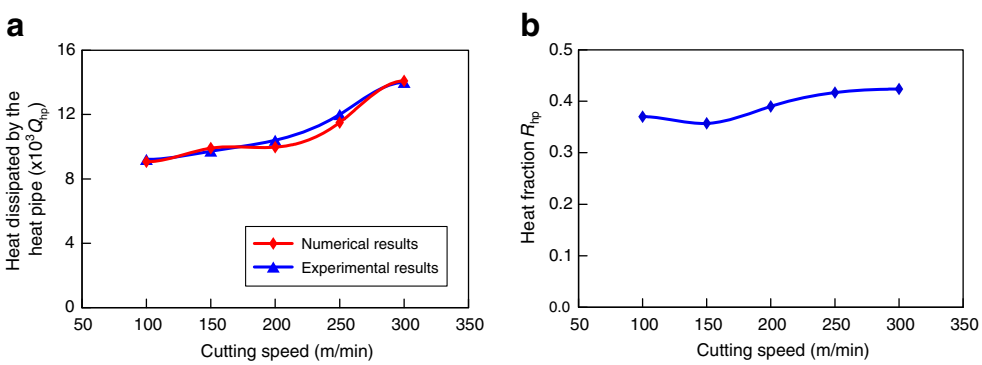

6 Conclusions

Based on the results and discussions presented in this paper, it can be concluded that:

1. Generally, in the same cutting condition, the average heat flux magnitude for the heat pipe cutter is higher than that of common cutter; however, the maximum temperature at tool–chip interface for the heat pipe cutter is significantly lower than that for the common cutter.
2. For both cutters, the heat partition into the cutting tool due to frictional heat source β decreases with the cutting speed. The value of β for the heat pipe cutter is higher than that for the common cutter in all cutting speed.
3. As for the heat pipe cutter, 36–42 % of the heat flowing into the tool can be dissipated through the heat pipe. Generally, the ratio of the heat dissipated by the heat pipe to the heat flowing into the cutting tool R_{hp} increases gradually with the cutting speed increase.
4. The installation of the heat pipe significantly reduces the heat retaining in the toolholder. As for the common cutter, the ratio of the heat retaining in the toolholder to the heat flowing into the cutting tool R_{th} is more than 90 %, while that for the cutter with heat pipe cooling is only 56–60 %.

Acknowledgments This task was supported by the National Nature Science Foundation of China with grant no. 50975094, China Postdoctoral Science Foundation with grant no.2012M511793, the Fundamental Research Funds for the Central University with grant no. 2012ZB0013, and the Open Fund of South China University of Technology with grant no. 2011009B.

References

1. Abukhshim NA, Mativenga PT, Sheikh MA (2005) Investigation of heat partition in high speed turning of high strength alloy steel. Int J Mach Tools Manuf 45:1687–1695. doi:10.1016/j.ijmachtools.2005.03.008
2. Sugiara T, Enomoto T (2011) Improving anti-adhesion in aluminum alloy cutting by micro stripe texture. Precis Eng 33:248–254. doi:10.1016/j.precisioneng.2011.10.002
3. Dosbaeva J, Rabinovich GF, Dasch J, Veldhuis S (2008) Enhancement of wet and MQL-based cutting of automotive alloys using cutting tools with DLC/polymer surface treatments. J Mater Eng Perform 17(3):346–351. doi:10.1007/s11665-008-9209-5
4. Faghri A (1995) Heat pipe science and technology. Taylor and Francis, Washington
5. Zhu L, Jen TC, Yin CL (2012) Experimental analyses to investigate the feasibility and effectiveness in using heat pipe-embedded drills. Int J Adv Manuf Technol 58:861–868. doi:10.1007/s00170-011-3436-x
6. Zhu L, Jen TC, Yin CL (2012) Investigation of the feasibility and effectiveness in using heat pipe-embedded drill by finite element analysis. Int J Adv Manuf Technol. doi:10.1007/s00170-012-4077-4
7. Jen TC, Gutierrez G, Eapen S, Barber G, Zhao H, Szuba PS, Labataille J, Manjunathaiah J (2002) Investigation of heat pipe cooling in drilling applications. Part I: preliminary numerical analysis and verification. Int J Mach Tools Manuf 42:643–652
8. Judd RL, Aftab K, Elbestawi MA (1995) An investigation of a heat pipe cooling system for use in turning on a lathe. Int J Adv Manuf Technol 10:357–366. doi:10.1007/BF01179398
9. Haq AN, Tamizharasan T (2006) Investigation of the effects of cooling in hard turning operations. Int J Adv Manuf Technol 30:808–816. doi:10.1007/s00170-005-0128-4
10. Chiou RY, Lu L, Chen JS-J, North MT (2007) Investigation of dry machining with embedded heat pipe cooling by finite element analysis and experiments. Int J Adv Manuf Technol 31:905–914. doi:10.1007/s00170-005-0266-8
11. Chou YR-K, Liu J (2005) CVD diamond tool performance in metal matrix composite machining. Surf Coat Technol 200:1872–1878. doi:10.1016/j.surfcoat.2005.08.094
12. Liang L, Quan YM, Ke ZY (2011) Investigation of tool–chip interface temperature in dry turning assisted by heat pipe cooling. Int J Adv Manuf Technol 54:35–34. doi:10.1007/s00170-010-2926-6
13. Liu J (2005) An investigation on cutting tool temperatures in machining of high-strength aluminum alloys and composites assisted with vortex-tube and heat-pipe cooling. PhD Dissertation of University of Alabama
14. Liang L (2011) Research on heat dissipation performance of heat pipe cutter for green machining. PhD Dissertation of South China University of Technology
15. Shaw MC (1984) Metal cutting principles. Oxford University Press, Oxford
16. Zhou ZH (1984) Metal cutting mechanism. Shanghai Science & Technology, Shanghai